Wideband Low Profile Multi-Polarization Reconfigurable Antenna with Quasi-cross-shaped Coupling Slot

Qun Xu [1,2], Zhiming Liu [1,3], Shaobin Liu [1*], Xiangkun Kong [1], Zhengyu Huang [1], Borui Bian [1], Qiming Yu [1], and Jianghong Qin [1]

[1] College of Electronic and Information Engineering
Nanjing University of Aeronautics and Astronautics, Nanjing, 211106, China
xuqun_jn@126.com, lzmedu@foxmail.com, lsb@nuaa.edu.cn*, xkkong@nuaa.edu.cn, huangzynj@nuaa.edu.cn, bbr@nuaa.edu.cn, yqm1604504@nuaa.edu.cn, 531416050@qq.com

[2] The Aeronautical Science Key Lab for High Performance Electromagnetic Windows
Country the Research Institute for Special Structures of Aeronautical Composite AVIC, Jinan, 250023, China

[3] Department of Electrical and Computer Engineering
University of Victoria, Victoria, BC, V8W 2Y2, Canada

Abstract ─ A wideband low profile multi-polarization reconfigurable antenna with quasi-cross-shaped coupling slot is proposed. The antenna consists of an upper oval radiating patch, the quasi-cross-shaped coupling slot, fork-shaped folded feed lines and a reconfigurable Wilkinson power divider network with four pairs of p-i-n diodes. The antenna reconfigurable polarization modes change among ±45° Linear polarization (LP), dual-LP, left-hand circular polarization (LHCP) and right-hand circular polarization (RHCP) by controlling the ON/OFF states of the p-i-n diodes. The designed prototype has been fabricated and measured. Good agreement between the measured and simulated results is achieved. Measured results show that the antenna has wide impedance bandwidth (over 21.35% for LP and 17.70% for CP) and axial ratio (AR) bandwidth (16.13% for LHCP and 16.88% for RHCP). The average realized gains are about 7.6 dBi for different polarization modes. The proposed antenna has the advantages of multi-polarization reconfigurable ability, wide bandwidth, low profile, and high gains, which make it possible to be applied to wireless communication systems.

Index Terms ─ Low profile, polarization reconfigurable antenna, slot antenna, wideband.

I. INTRODUCTION

Operating characteristics of antennas affect directly the performances of wireless communication systems. With the development of technology, wireless communication systems have been applied to different requirements of wireless services, which causes the limited electromagnetic spectrum resources becoming more and more crowded [1-4]. So, multiple wireless systems are required to be integrated into a single platform for maximum link-up. Therefore, a new generation of antennas that can be adjusted automatically according to environment changes is required.

Reconfigurable antennas not only reduce the size, weight and cost, but also enable the antenna to work in multiple frequency bands and have multiple modes of operation [5-7]. Polarized reconfigurable antennas are the focus of researches on reconfigurable antennas. They can improve the spatial freedom in limited space, which greatly improve the transmission rate and system capacity [8-10]. There are several types of polarizations used in antenna applications: vertical polarization (VP), horizontal polarization (HP), ±45° oblique polarization, [10,11], LHCP and RHCP [12-15]. The first four polarization belongs to LP. Compared with the traditional antennas, the polarization reconfigurable antennas have unparalleled advantages in frequency multiplexing and improving the performance of the polarization control system.

Nowadays, there are mainly two methods to realize electrically controlled polarization reconfiguration: One is to alter feeding network, and the other is to introduce reconfigurability on the radiating elements. The former one achieves the reconfiguration by loading variable reactance to the feeding network or switching the feeding position to generate the phase difference between different operating modes [10, 16, 17]. The latter one is to etch the gap on the proper position of the radiator, which uses RF switches to change the antenna current flow path and generate the phase difference [18-21]. However, most of the proposed antennas have a narrow bandwidth

Submitted On: September 10, 2019
Accepted On: February 23, 2020

especially for the LP and CP polarized reconfigurable antennas. The appearance of the narrow bandwidth is due to two orthogonal LP radiations with same amplitude produce CP mode, while the input impedances between the two LP and CP are different, which will cause the impedance mismatch for LP and CP. Furthermore, it is much harder to overlap the impedance bandwidth and 3-dB AR bandwidth in the broadband range.

In this paper, a novel wideband low profile multi-polarization reconfigurable slot antenna with high realized gains is proposed. The antenna is composed of an upper oval radiating patch, the quasi-cross-shaped coupling slot, fork-shaped folded feed lines and a reconfigurable Wilkinson power divider network with four pairs of p-i-n diodes, which are introduced to change the current flow path to realize the reconfigurable among ±45° oblique LP, dual-LP (VP and HP), LHCP and RHCP. The impedance bandwidth and 3-dB axial-ratio bandwidth are almost overlapped for CP. Also, the average realized gain of the proposed antenna is higher than most of the other reported antennas.

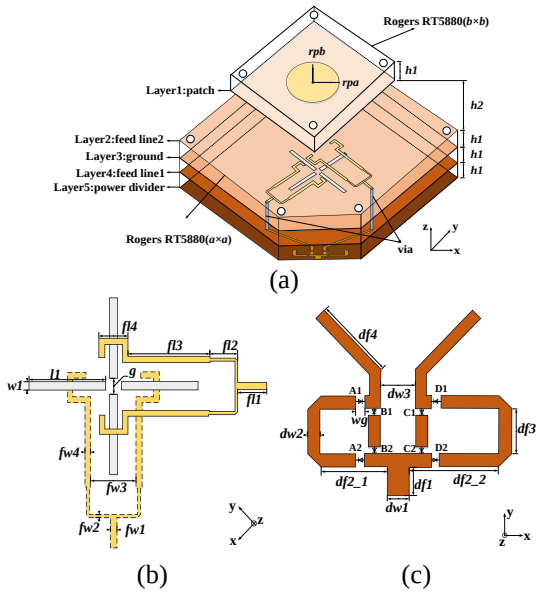

Fig. 1. Structure of the proposed multi-polarization reconfigurable antenna. (a) 3D, (b) Quasi-cross-shaped coupling slot with fork-shaped folded feed lines, and (c) Reconfigurable Wilkinson power divider network.

II. ANTENNA STRUCTURE AND OPERATING PRINCIPLE

The proposed antenna has a multi-layer structure, which consists of four substrates stacked together by nylon screws, and the plastic washers act as a support between the first two layers of substrates as shown in Fig. 1(a). All the substrates are the 0.508-mm thick Rogers RT5880 with a relative permittivity of 2.2 and a loss tangent of 0.0009. The dimensions of the proposed antenna are listed in Table 1.

Table 1: Parameters of the proposed antenna

Parameter	Value (mm)	Parameter	Value (mm)
a	140	*fl4*	7.5
b	80	*w1*	2
h1	0.508	*l1*	19.8
h2	8	*g*	4
rpa	21	*dw1*	3.2
rpb	20	*dw2*	1.8
fw1	1.58	*dw3*	5
fw2	0.9	*df1*	4
fw3	12.65	*df2_1*	10.2
fw4	1.25	*df2_2*	12.6
fl1	4	*df3*	6.4
fl2	7.5	*df4*	36
fl3	24.5	*wg*	0.9

A. Slot antenna

The design of the quasi-cross-shaped coupling slot antenna is based on the antenna proposed in [22]. As shown in Fig. 1 (b), the quasi-cross-shaped coupling slot is etched on the ground which consists of four separated rectangular slots arranged by rotating 90° in turn. The space between two parallel slots reduces the impurity of two linear polarizations and the coupling between two orthogonal polarizations in the center effectively. The fork-shaped folded feed lines are placed on the upper layer and lower layer of the ground plane which avoid the unwanted couplings among the feed line to feed line and feed lines to slots. The purity of two linear polarizations can be improved with the quasi-cross-shaped coupling slot and fork-shaped folded feed lines which provides great help for generating wideband circular polarization. Moreover, the antenna gain is higher than normal slot antennas due to the surface current intensity distributed in the middle and edges of the feed lines is in the same direction which increases the far-field radiation. Besides, the upper oval patch and air gap make a great contribution to the antenna bandwidth, gain and directivity.

B. Reconfigurable Wilkinson power divider network

The structure diagram of Wilkinson power divider with two output ports is shown in Fig. 2. Z_0 is the characteristic impedance of the input port, R_2 and R_3 are the load impedance. Assuming the ratio of output power is $1/k^2$, then:

$$\frac{1}{Z_{in2}}+\frac{1}{Z_{in3}}=\frac{1}{Z_0}, \tag{1}$$

$$k^2=\frac{P_3}{P_2},\ P_2=\frac{U_2^2}{2R_2},\ P_3=\frac{U_3^2}{2R_3},\ U_2=U_3. \tag{2}$$

According to $\lambda/4$ impedance transformation theory, there are:

$$Z_{in2} \times R_2 = Z_{02}^2, \quad (3)$$

$$Z_{in3} \times R_3 = Z_{03}^2. \quad (4)$$

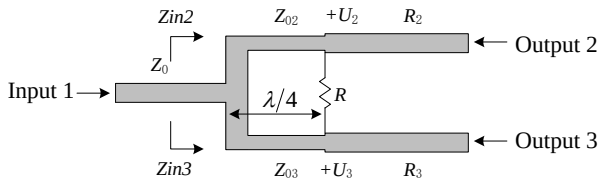

Fig. 2. The structure diagram of Wilkinson power divider with two output ports.

Suppose $R_2 = kZ_0$, then,

$$Z_{02} = Z_0\sqrt{k(1+k^2)}, \; Z_{03} = Z_0\sqrt{\frac{(1+k^2)}{k^3}}, \quad (5)$$

$$R_3 = \frac{Z_0}{k}. \quad (6)$$

The resistance of the isolation resistor R can be expressed as:

$$R = Z_0(k + \frac{1}{k}). \quad (7)$$

When k=1, ports 2 and 3 output the same power signal, $Z_{02} = Z_{03} = \sqrt{2}Z_0$, and the resistance of the isolation resistor is R=2Z_0. In order to reduce the size of the Wilkinson power divider, a Wilkinson power divider network with two λ/4 transmission lines is designed for realizing the polarization reconfiguration, and the schematic is shown in Fig. 1 (c). The network provides phase shifts on different branches by etching separated microstrip lines of different lengths. The microstrip line 2 and line 3 with the same size are located in the middle of the four branches, while the outside microstrip line 1 and line 4 are about λ/4 longer than the inside ones, λ is the guided wavelength at the resonant frequency. The two output ports of the Wilkinson power divider network are connected to the upper feed lines through the vias. Since the upper feed lines are placed on the different layers of the ground plane and the distances to output ports are different, the power divider asymmetric which means the microstrip line 1 is longer than the line 4. Four pairs of p-i-n diodes (A1 and A2; B1 and B2; C1 and C2; D1 and D2) are placed in four different branches respectively to connect the branches with the output ports. By controlling the diodes on and off, different branches can be chosen to generate the phase difference of 0° or ±90°. When diode groups A and C are switched on and others are off, the microstrip line 1 generates a 90° phase delay than the line 3, then the RHCP can be achieved. Similarly, diode groups B and D switched on and others off, the LHCP can be generated. LP can be achieved when just one pair of p-i-n switch on, but only when the diode group A or D switch on could result in a better impedance match. In addition, the ±45° orthogonal dual-LP with high isolation and purity can be generated when diode groups B and C switched on and others off. The corresponding relationship between the diode states and the antenna polarization modes are shown in Table 2. It should be noted that the LP directions are ±45° which is the angle with the positive x-axis.

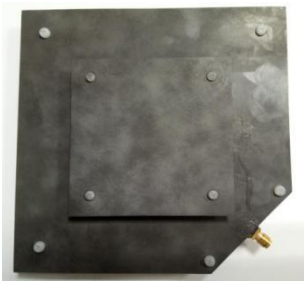

Fig. 3. Photograph of the fabricated antenna.

Table 2: The corresponding relation between diode state and antenna polarization mode

Polarization Mode	Diode State			
	p-i-n A	p-i-n B	p-i-n C	p-i-n D
State 1: +45° LP	ON	OFF	OFF	OFF
State 2: -45° LP	OFF	OFF	OFF	ON
State 3: dual-LP	OFF	ON	ON	OFF
State 4: LHCP	OFF	ON	OFF	ON
State 5: RHCP	ON	OFF	ON	OFF

III. RESULTS AND DISCUSSION

The designed prototype has been fabricated and measured. The simulated and measured results are presented. Figure 3 shows the photograph of the fabricated antenna. The 8 mm M3 nylon bolts are used to support the first layer of the substrate. The simulated results are obtained by CST2017. In the simulation process, the waveguide port was used for feeding, the boundary conditions use open (add space) in all directions, and the time domain solver was applied. The p-i-n diode SMP1345-79 [23] is chosen to connect the different branches of the Wilkinson power divider network. Based on the diode datasheet, the diode is modelled as a 2 Ω resistor for the ON-state and a parallel circuit of a 0.15 pF capacitor and 8000 Ω resistor for the OFF-state. All measurements were performed in a microwave anechoic chamber.

The measured and simulated reflection coefficients for all the modes are shown in Fig. 4. It is observed that the measured 10-dB impedance bandwidths covered wide frequency bands from 2.76 to 3.51 GHz (0.75 GHz, 23.92%) for +45° LP, 2.66 to 3.40 GHz (0.74 GHz, 24.42%) for -45° LP, 2.72 to 3.37 GHz (0.65 GHz, 21.35%) for dual-LP, 2.78 to 3.32 GHz (0.54 GHz, 17.70%) for LHCP and 2.86 to 3.52 GHz (0.66 GHz, 20.69%) for RHCP. The external bias circuit for p-i-n

diodes caused the differences between measured and simulated results. Furthermore, the loading changed since the actual value of the equivalent circuit of the p-i-n diodes may differ from the labeled value. The fabrication and measurement tolerance also affected the results.

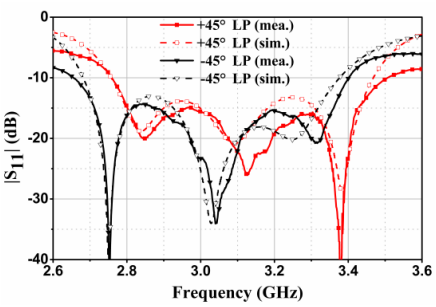

(a)

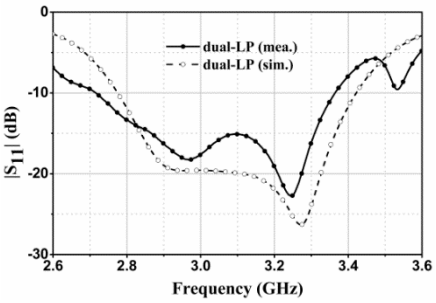

(b)

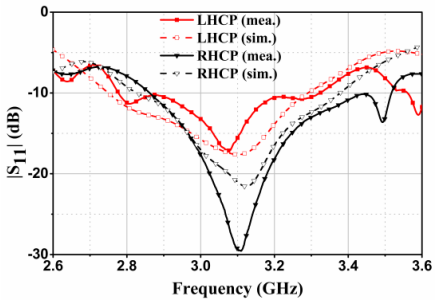

(c)

Fig. 4. Measured and simulated reflection coefficients for all modes: (a) ±45° LP, (b) Dual-LP, and (c) CP.

Figure 5 shows the measured and simulated realized gains of the antenna for LP modes and Fig. 6 presents the realized gains and axial ratios for CP modes which indicates great agreements. It can be seen that the antenna realized gains are quite stable along the operating bandwidth, while the measured peak gains are 8.45 dBi for LP and 8.36 dBi for CP, and the average gains are 7.63 dBi for LP and 7.61 dBi for CP over impedance bandwidth. The measured 3-dB AR bandwidths are 2.85 to 3.35 GHz (0.48 GHz, 16.13%) for LHCP and 2.82 to 3.34 GHz (0.48 GHz, 16.88%) for RHCP, which are wider than most of the proposed polarized reconfigurable antennas.

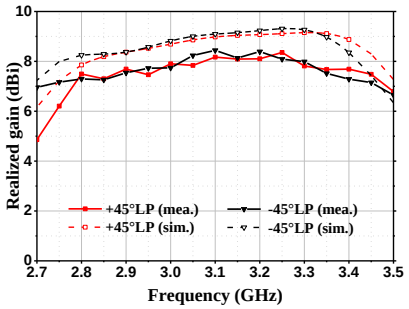

Fig. 5. Measured and simulated realized gains for LP modes.

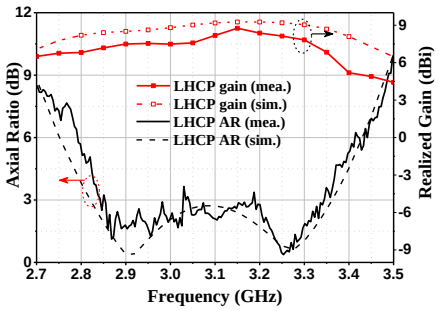

(a)

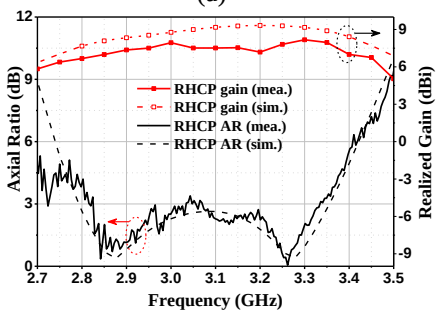

(b)

Fig. 6. Measured and simulated realized gains and axial ratios for CP modes: (a) LHCP and (b) RHCP.

The measured and simulated normalized radiation patterns for LP and CP modes at 2.8, 3.0 and 3.3 GHz are shown in Figs. 7-9. It is observed from Fig. 7 and Fig. 8 that the patterns of the two orthogonal cut-planes (φ=+45° plane and φ=-45° plane) are compared for +45° LP and -45° LP. CP patterns are shown in Fig. 8. The measured cross-polarization levels for all modes are almost below -15 dB. A larger back lobe and unexpected side lobes are found in the measured radiation patterns which are caused by the test environment and affected by the p-i-n diodes with the bias circuit and external DC power device.

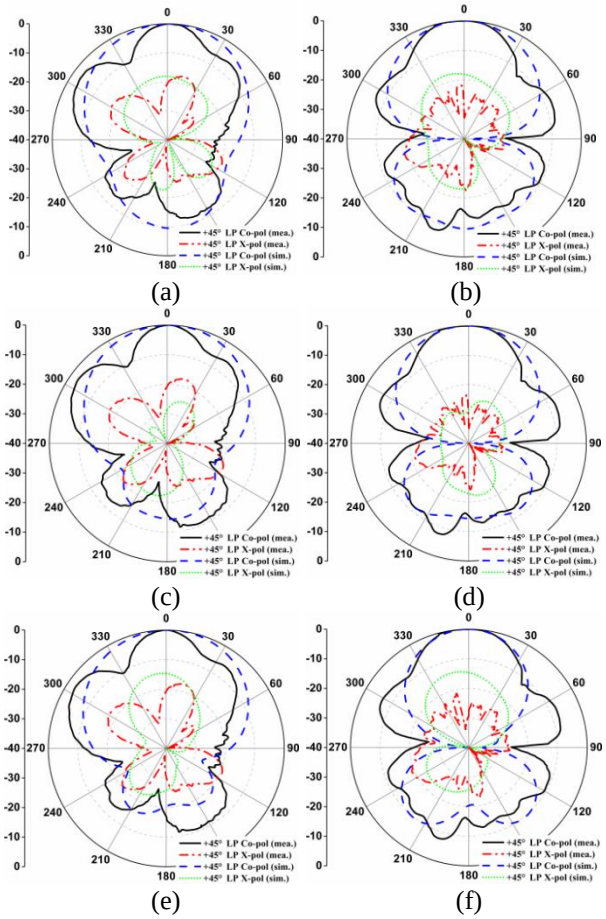

Fig. 7. Measured and simulated radiation patterns for +45° LP mode. (a) φ=+45° and (b) φ=-45° planes at 2.8 GHz, (c) φ=+45° and (d) φ=-45° planes at 3.0 GHz, (e) φ=+45° and (f) φ=-45° planes at 3.3 GHz.

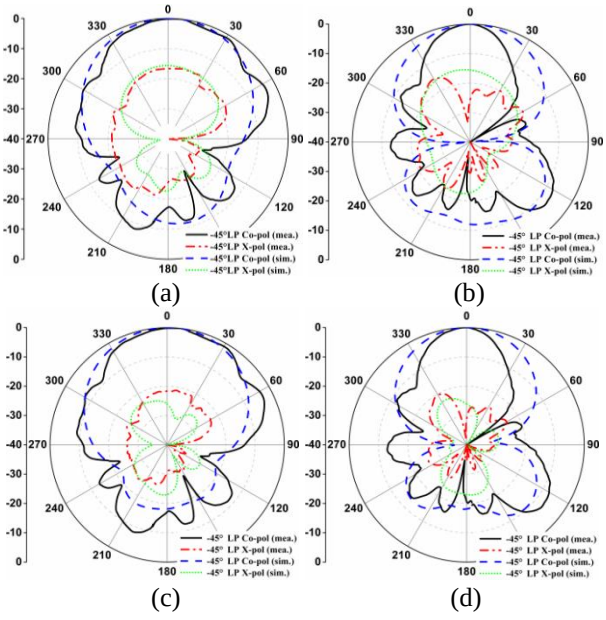

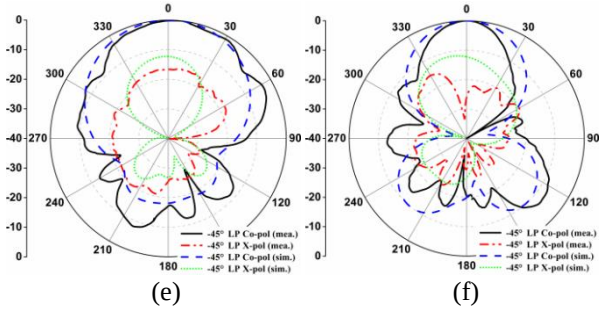

Fig. 8. Measured and simulated radiation patterns for -45° LP mode. (a) φ=-45° and (b) φ=+45° planes at 2.8 GHz, (c) φ=-45° and (d) φ=+45° planes at 3.0 GHz, (e) φ=-45° and (f) φ=+45° planes at 3.3 GHz.

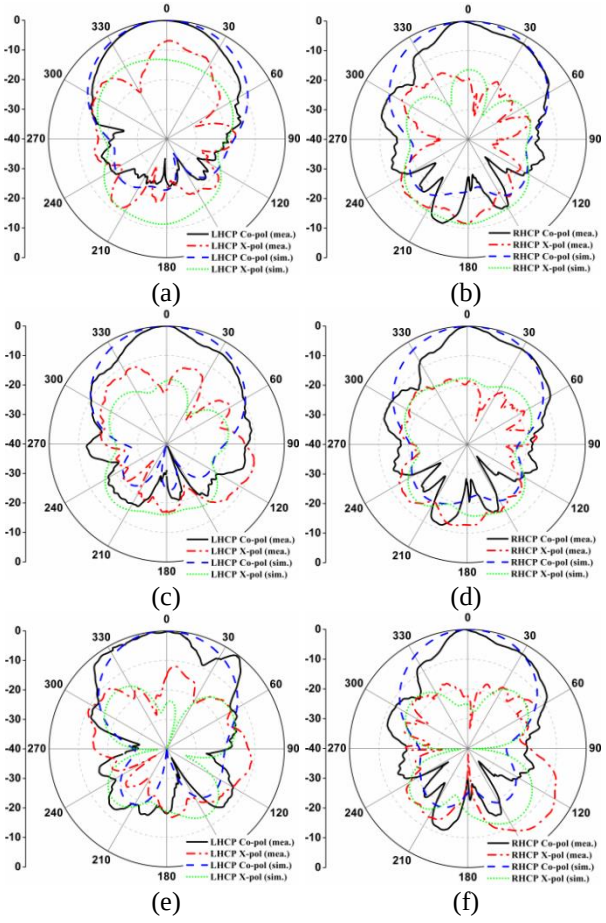

Fig. 9. Measured and simulated radiation patterns for CP modes. (a) LHCP and (b) RHCP at 2.8 GHz, (c) LHCP and (d) RHCP at 3.0 GHz, (e) LHCP and (f) RHCP at 3.3 GHz.

Finally, Table 3 gives the comparisons among reported polarization reconfigurable antennas and the proposed antenna. It can be concluded that the proposed polarization reconfigurable antenna realized wide

impedance bandwidth, AR bandwidth, high realized gains and low profile with five polarization modes.

Table 3: Comparison with reported polarization reconfigurable antennas

0	Polarization States	IMBW (%)	ARBW (%)	Height
[1]	LP LHCP/RHCP	14.2 26.4	- 13.5	$0.60\lambda_0$
[9]	LHCP RHCP	80	37.8 26.9	$0.32\lambda_0$
[14]	LP LHCP/RHCP	27.2 21.9	- 23.5	$0.27\lambda_0$
[22]	LP LHCP/RHCP	7.3	- 1.5	$0.043\lambda_0$
[23]	HP/VP LHCP/RHCP	20 25.6	- 4	$0.10\lambda_0$
Pro.	±45° LP/dual-LP LHCP/RHCP	>23.9 >17.7	- 16.1/16.9	$0.11\lambda_0$

VI. CONCLUSION

A wideband low profile multi-polarization reconfigurable slot antenna with high realized gains has been presented. Four pairs of p-i-n diodes which are placed in four different branches of the reconfigurable Wilkinson power divider network controlling the antenna reconfigurable polarization modes among ±45° LP, dual-LP, LHCP and RHCP. The upper slot antenna with fork-shaped folded feed lines provides two pure orthogonal linearly polarizations, which makes great help for generating wideband circular polarization. The designed prototype was fabricated and measured, showing agreement between the measured and simulated results. Compared to most of the reported antennas, wider impedance bandwidths (over 21.35% for LP and 17.70% for CP) and AR bandwidths (16.13% for LHCP and 16.88% for RHCP) with high realized gains ~7.6 dBi are obtained. Finally, the proposed antenna has the advantages of multi-polarization reconfigurable ability, wide bandwidth, low profile and high gains, which make it possible to be applied to wireless communication systems.

ACKNOWLEDGMENT

This work was supported in part by Chinese Natural Science Foundation (Grant Nos. 61671238; 61471368; 61901217), in part by the Fundamental Research Funds for the Central Universities (No. NJ20160008), in part by Natural Science Foundation of Jiangsu Province (Grant No. BK20190406) in part by China Postdoctoral Science Foundation (Grant Nos. 2016M601802; 2019M661829), in part by the Equipment Advanced Research Foundation of China (Grant No. 61402090103), in part by Jiangsu Planned Projects for Postdoctoral Research Funds (Grant No. 1601009B; 2019K018A), and in part by Aeronautical Science Foundation of China (20161852016). Zhiming Liu greatly acknowledges funding from the China Scholarship Council (CSC) for Grant 201906830035.

REFERENCES

[1] L. Y. Ji, P. Y. Qin, Y. J. Guo, C. Ding, G. Fu, and S. X. Gong, "A wideband polarization reconfigurable antenna with partially reflective surface," *IEEE Trans. Antenna Propag.*, vol. 64, no. 10, pp. 4534-4538, Oct. 2016.

[2] Z.-C. Hao, H.-H. Wang, and W. Hong, "A novel planar reconfigurable monopulse antenna for indoor smart wireless access points' application," *IEEE Trans. Antenna Propag.*, vol. 64, no. 4, pp. 1250-1261, Apr. 2016.

[3] J. S. Row, and M. J. Hou, "Design of polarization diversity patch antenna based on a compact reconfigurable feeding network," *IEEE Trans. Antenna Propag.*, vol. 62, no. 10, pp. 5349-5352, Oct. 2014.

[4] H. Sun and S. Sun, "A novel reconfigurable feeding network for quad-polarization-agile antenna design," *IEEE Trans. Antenna Propag.*, vol. 64, no. 1, pp. 311-316, Jan. 2016.

[5] Z. C. Hao, K. K. Fan, and H. Wang, "A planar polarization-reconfigurable antenna," *IEEE Trans. Antenna Propag.*, vol. 65, no. 4, pp. 1624-1632, Apr. 2017.

[6] M. N. Osman, M. K. Abdul Rahim, M. R. Hamid, M. F. M. Yusoff, and H. A. Majid, "Compact dual-port polarization-reconfigurable antenna with high isolations for MIMO application," *IEEE Antennas Wireless Propag. Lett.*, vol. 15, pp. 456-459, July 2016.

[7] S. W. Lee and Y. J. Sung, "Simple polarization-reconfigurable antenna with T-shaped feed," *IEEE Antennas Wireless Propag. Lett.*, vol. 5, pp. 114-117, 2016.

[8] J.-F. Tsai and J.-S. Row, "Reconfigurable square-ring microstrip antenna," *IEEE Trans. Antennas Propag.*, vol. 61, no. 5, pp. 2857-2860, 2013.

[9] H. Wong, W. Lin, L. Huitema, and E. Arnaud, "Multi-polarization reconfigurable antenna for wireless biomedical system," *IEEE Trans. Biomedical Circuits Syst.*, vol. 11, no. 3, pp. 652-660, 2017.

[10] S.-L. Chen, F. Wei, P.-Y. Qin, Y. Jay Guo, and X. Chen, "A multi-linear polarization reconfigurable unidirectional patch antenna," *IEEE Trans. Antenna Propag.*, vol. 65, no. 8, pp. 4299-4304, 2017.

[11] L. Ge, X. J. Yang, D. G. Zhang, M. J. Li, and H. Wong, "Polarization-reconfigurable magneto-electric dipole a cv antenna for 5G Wi-Fi," *IEEE Antennas Wireless Propag. Lett.*, vol. 16, pp. 1504-1507, 2017.

[12] W. Lin and H. Wong, "Wideband circular

polarization reconfigurable antenna," *IEEE Trans. Antenna Propag.*, vol. 63, no. 12, pp. 5938-5944, 2015.

[13] D. Piazza, J. Kountouriotis, M. D'Amico, and K. R. Dandekar, "A technique for antenna configuration selection for reconfigurable circular patch arrays," *IEEE Trans. Wireless Commun.*, vol. 8, no. 3, pp. 1456-1467, 2009.

[14] M. Fakharian, P. Rezaei, and A. A. Orouji, "Reconfigurable multiband extended U-slot antenna with switchable polarization for wireless applications," *IEEE Antennas Propag. Mag.*, vol. 57, no. 2, pp. 194-202, Apr. 2015.

[15] J. S. Row, W. L. Liu, and T. R. Chen, "Circular polarization and polarization reconfigurable designs for annular slot antennas," *IEEE Trans. Antennas Propag.*, vol. 60, no. 12, pp. 5998-6002, 2012.

[16] W. Lin and H. Wong, "Polarization reconfigurable wheel-shaped antenna with conical-beam radiation pattern," *IEEE Trans. Antennas Propag.*, vol. 63, no. 2, pp. 491-499, 2015.

[17] J. Hu, Z.-C. Hao, and W. Hong, "Design of a wideband quad-polarization reconfigurable patch antenna array using a stacked structure," *IEEE Trans. Antennas Propag.*, vol. 65, no. 6, pp. 3014-3023, 2017.

[18] M. S. Nishamol, V. P. Sarin, D. Tony, C. K. Aanandan, P. Mohanan, and K. Vasudevan, "An electronically reconfigurable microstrip antenna with switchable slots for polarization diversity," *IEEE Trans. Antennas Propag*., vol. 59, no. 9, pp. 3424-3427, 2011.

[19] A. Khidre, K.-F. Lee, F. Yang, and A. Z. Elsherbeni, "Circular polarization reconfigurable wideband E-shaped patch antenna for wireless applications," *IEEE Trans. Antennas Propag*., vol. 61, no. 2, pp. 960-964, 2013.

[20] Z.-X. Yang, H.-C. Yang, J.-S. Hong, and Y. Li, "Bandwidth enhancement of a polarization-reconfigurable patch antenna with stair-slots on the ground," *IEEE Antennas Wireless Propag. Lett.*, vol. 13, pp. 579-582, 2014.

[21] K. M. Mak, H. W. Lai, K. M. Luk, and K. L. Ho, "Polarization reconfigurable circular patch antenna with a C-shaped," *IEEE Trans. Antennas Propag.*, vol. 65, no. 3, pp. 1388-1392, 2017.

[22] J. Lu, Z. Q. Kuai, X. W. Zhu, and N. Z. Zhang, "A high-isolation dual-polarization microstrip patch antenna with quasi-cross-shaped coupling slot," *IEEE Trans. Antennas Propag.*, vol. 59, no. 7, pp. 1713-2717,2011.

[23] Skyworks Datasheet for SMP1345. [Online]. Available: https://www.skyworksinc.com/en/Products/Diodes/SMP1345-Series.